Morphological aspects of recurrent prostate cancer

Rybalov, Maxim

Chapter 2

Does CT or PET/CT contribute to detection of small focal cancers in the prostate?

Li MM, Rybalov M, Haider MA, de Jong IJ.

J Endourol. 2010 May;24(5):693-700.

ABSTRACT

Prostate cancer is considered to be a multifocal tumor in the majority of patients. Based on histologic data after prostatectomy, there is a growing insight that a considerable number of men who receive a diagnosis in the contemporary setting of prostate-specific antigen screening have unilateral or unifocal disease. With this, the current concept of whole-gland therapy has come into discussion. The need for improvement of intraprostatic tumor characterization is clear. Molecular imaging is one of the areas of research on this aspect. The clinical indications for positron emission tomography (PET)/CT have increased rapidly in the field of oncology and are largely based on fluorodeoxyglucose (FDG) PET. Both conventional CT and FDG PET, however, cannot detect prostate cancer foci <5 mm within the prostate. Dynamic contrast-enhanced CT involves imaging a region of interest rapidly (usually <10 seconds between images) during a bolus intravenous injection of a contrast agent. Through analysis of the contrast enhancement time curves, it is possible to distinguish tissues with different microvascular properties such as cancer. The technologic aspects of both imaging techniques and the clinical results of ^{11}C-choline PET/CT for intraprostatic tumor characterization are discussed.

Based on preliminary studies, dynamic contrast-enhanced (DCE)-CT may be a useful tool for localization of prostate tumors and, perhaps more importantly, quantification of therapeutic response in prostate cancer. Validation work is necessary, however, to define its accuracy and role in therapeutic paradigms such as focal therapies, particularly given the current accuracy of MRI. In the future, combining DCE-CT with CT or ^{11}C-choline PET/CT may be an alternative to MRI, offering a combination of quantitative parameters that may correlate to tumor prognosis as well as cancer localization for focal therapy.

INTRODUCTION

According to current EUA and AUA guidelines, CT alone is not recommended for the staging of newly diagnosed cancer as it is not sufficiently reliable for the assessment of local T-staging.[1] CT shows limited sensitivity (30-50%) and overall accuracy of 67-70%[2, 3]. Because of the extremely low likelihood of positive findings in new patients with a PSA < 20 ng/mL (1%) or with a Gleason score < 8 (1.2%), guidelines state that CT is only indicated in patients in advanced stages who are likely to have lymph node findings present.[1] In particular, CT may be considered when PSA > 20 ng/mL or when the Gleason score is ≥ 8.[5] CT planning is recommended for external beam radiotherapy.[1, 5] In particular, the AUA recommends CT in combination with a bone scan for external beam patients with a Gleason score ≥8 or PSA level >20 ng/mL.[5] In addition, multiple CT scans may be of value in determining prostate motion during the course of this therapy.[6] Preliminary research also shows that regular CT scans holds promise as a tool for improved tumour targeting and prostate positioning during image-guided intensity-modulated radiotherapy (IMRT).[7, 8]. The guidelines on the indications for PET in prostate cancer have not been defined. In this article we review the recent developments in visualization and localization of prostate cancer using Dynamic Contrast Enhanced CT and PET/CT.

LOCALIZATION OF PROSTATE CANCER WITH DYNAMIC CONTRAST ENHANCED CT (DCE-CT)

Dynamic contrast enhanced imaging, sometimes referred to as “perfusion imaging” involves imaging a region of interest rapidly (usually <10s between images) during a bolus intravenous injection of a contrast agent.[11] Through analysis of the contrast enhancement time curves it is possible to distinguish tissues with different microvascular properties (Figure 1). Angiogenesis has been known to be an important process in the growth, proliferation and metastasis of cancers[11, 12]. Most tumours, including prostate cancer, exhibit alterations in permeability and microvessel density when compared to the normal peripheral zone.[13] DCE-MRI studies have shown prostate cancer typically exhibits higher peak enhancement and washout compared to the surrounding normal gland [14]. This has been most studied in whole mount correlation studies with DCE-MRI showing good localization specificities (88-97%) and accuracies (87-92%).[15-17] This differential enhancement of prostate cancer suggested a properly timed helical CT may allow for cancer depiction with CT.[18]

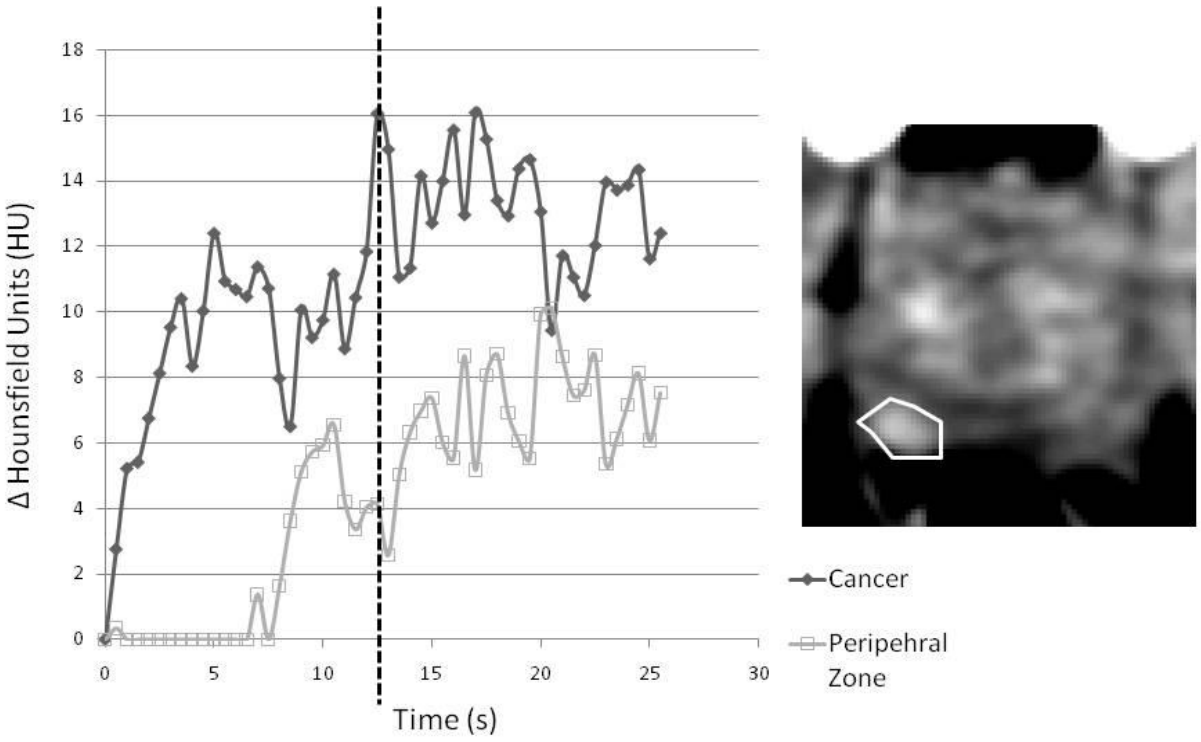

Fig 1 DCE-CT.

Dynamic CT images were acquired at 0.5s intervals after injection of intravenous contrast. Graph shows change in attenuation from baseline for cancer region of interest (white outline) and normal peripheral zone. The image is a single slice at 13s after onset of contrast enhancement (vertical dotted line) in the prostate. Note how the tumor (Gleason 4+3) enhances earlier and has a higher peak enhancement than normal peripheral zone. Benign transition zone nodules (central bright regions) can also exhibit enhancement patterns similar to cancer making diagnosis of cancers in this region difficult.
Source DCE CT data for this case courtesy of C Miller, T Wong TJ Polascik and V Mouraviev, Duke University Medical Center, Durham, NC, USA

One may ask why DCE-CT has not been more extensively used. CT is more readily available at most centers and is used routinely in radiation therapy planning.[1, 5] Successful localization of tumour with DCE-CT would avoid the need for MRI-CT registration for delivering tumour targeted radiation therapy. In the past DCE-CT has been difficult to perform in the prostate because of limited coverage with scanners only able to cover 2cm of tissue. This has been remedied by the development of 64 slice and 320 slice scanners which

allow for coverage of up to 16 cm of tissue.[11, 19] Radiation dose and the associated cancer risk remains a concern with DCE-CT compared to MRI as the latter involves no ionizing radiation.

In particular, typical abdominal CT radiation doses range from 10-20 mSV where a single 10 mSV dose is associated with a lifetime developmental risk of 0.1% for a solid cancer or leukemia[20] and a 0.01-0.14% lifetime attributable risk of death from cancer[21]. It should be noted that these effect is heavily age-dependent: for example, by age 50, the lifetime attributable risk of death from cancer is less than 0.02%.[21] A promising role for DCE-CT may be for prostate cancer localization for improving outcomes in radiation therapy through dose escalation to the dominant tumour focus[1, 5] as the radiation dose for DCE-CT is relatively minimal compared to a therapeutic dose, and collateral radiation exposure is associated with an increased risk of non-prostatic cancer post-treatment.[22]

The inherent value of DCE-CT for prostate cancer may lie in its ability to quantify vascular properties of the cancer.[13] For each voxel in the image a curve of contrast enhancement versus time can be plotted. This curve can be analyzed using semi-quantitative methods to derive parametric maps such as peak enhancement, area under the enhancement curve (IAUC), maximum slope and washout rate.[23, 24] Alternatively a pharmacokinetic models based on the assumed contrast kinetics of the tissue microvasculature can be used to derive more physiologic parameters such as vascular permeability, blood volume and blood flow (Figure 2).[11]

Using the images from the case shown in Fig 1, parametric images of the microvasculature related parameters (bottom row) were generated on a voxel by voxel basis using CT Perfusion 4 software (GE Healthcare, Waukesha, WI, USA). DCE-CT image through the prostate apex shows a focal region of cancer (white arrows) exhibit elevated blood flow, permeability surface area product and blood volume compared to normal peripheral zone. The transition zone nodules can behave like cancers exhibiting increase blood flow and permeability.

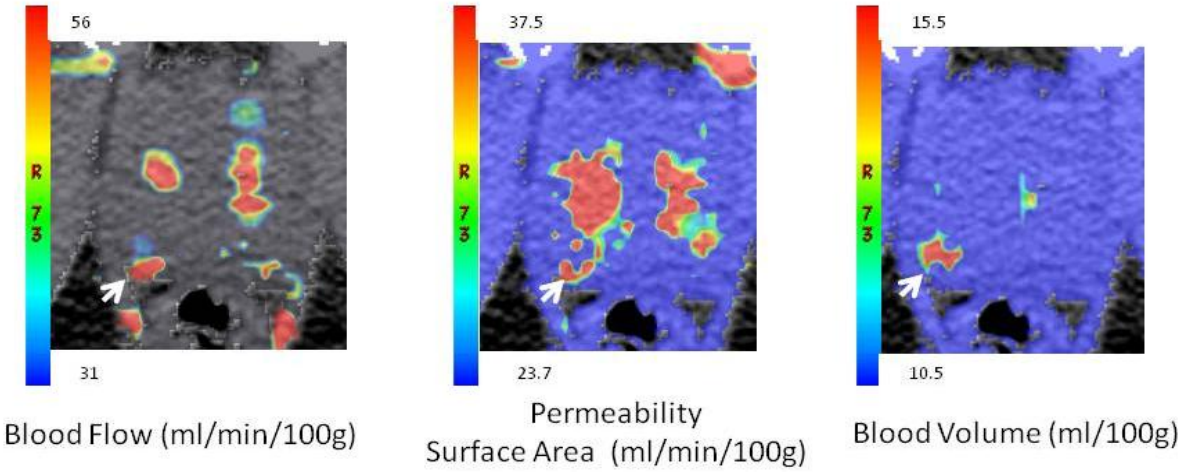

Fig 2 Right apex Gleason 7 (4+3) cancer seen with Pharmacokinetic Analysis of DCE-CT.

Source DCE CT data for this case courtesy of C Miller, T Wong TJ Polascik and V Mouraviev, Duke University Medical Center, Durham, NC, USA

While both DCE-CT and dynamic contrast-enhanced MRI (DCE-MRI) may be used to determine functional parameters such as blood flow (BF), blood volume (BV), mean transit times (MTT) and capillary permeability (PS), there are distinct advantages and disadvantages to each of the two modalities when it comes to pharmacokinetic modeliing.[11-13] In particular, analysis of DCE-CT data is significantly easier, as a direct linear relationship exists between the enhancement observed (measured in Hounsfield units, HU) and the concentration of contrast material injected, which allows for the exact quantification of the arterial input function.[11, 25] In contrast, the MRI signal change not only varies non-linearly with contrast dose but also varies with intrinsic relaxation rates, tissue inhomogenities and even the pulse sequence used.[11] However, DCE-CT suffers from a relatively poorer signal-to-noise ratio as compared to DCE-MRI, which may limit detection of small cancers.[11, 13, 25] The use of DCE-CT to measure parameters of angiogenesis has shown validation with diverse paradigms, including the microsphere method (r = 0.84-0.96) [26, 27], $H_2{}^{15}O$ PET (r = 0.72)[28] and measurements of VEGF level[29]. DCE-CT-measured BF also shows moderate correlation with histological measurements of MVD (r = 0.44-0.62)[30] and of calculated pO_2 in tumours (r = 0.47).[31] The evidence for DCE-CT reproducibility and repeatability have been mixed and both tissue type and the method of analysis may influence these factors; in addition, studies have not been done for DCE-CT use in the prostate.[29] Studies in other organs have suggested interscan variations of 13%-33% and values for within-subject coefficients of variation (wCV) ranging from 12-47%.[25, 32] Correlation coefficients (Pearson r) for inter-observer reproducibility in similar studies are high (0.80-0.94) and a study

comparing two analysis methods (slope and deconvolution), showed values ranging from r = 0.86-0.90, suggesting that there is good inter-technique validity as well.[25]

There are limited studies in the use of DCE-CT in the prostate. A preliminary study by Prando *et al.* showed a simple single time point helical CT obtained 50s after a contrast injection can depict larger and more vascular cancers with an accuracy of 58%.[18] This is fairly similar to transrectal ultrasound (accuracies of 50-63%)[33, 34] so a single time point scan is likely inadequate for adoption for planning of focal therapies. Henderson *et al.* used the adiabatic approximation of the tissue homogeneity model (modelling tracer kinetics) using high temporal resolution DCE CT (1s) to create parametric maps of the prostate allowing for calculations of normal prostatic BF (0.18±0.05ml/min/g), PS (0.17±0.06ml/min/g), MTT (49±8s) and BV (0.09±0.02ml/g).[24, 35] These were significantly different from presumed tumour 'hot spots' (BF: 0.37±0.12ml/min/g, PS: 0.24±0.10, MTT: 41±16s and BV: 0.17±0.06ml/g). A recent follow-up study by Jeukens *et al.* used a multi-slice DCE-CT protocol to image the entire prostate using 2 scans and similarly analyzed the data using the adiabatic approximation of the tissue homogeneity model.[23]

Encouragingly, similar BF calculations were obtained for both normal prostate (0.10-17ml/min/g) and tumourous tissue (0.29-0.45ml/min/g) in comparison to Henderson's study.[23, 24] It was shown that at a noise level of ~4 HU, one can sufficiently (95% confidence interval) detect a deviation of a parameter from a given threshold using this model.[23] This noise level can be achieved with a voxel size of 9 x 9, which corresponds to a volume of ~0.1ml.[23] The authors suggest that this is of high enough spatial resolution to detect small and large, and irregular-shaped cancers of the prostate.[23] Whole mount correlation studies showing the accuracy of DCE-CT for localization of prostate cancer are lacking at the time of this review.

Because DCE-CT lends itself to measurements of blood flow, permeability and blood volume, it may be a useful tool in the measurement of the radiotherapy response.[36, 37] Harvey *et al.* used DCE-CT to measure a number of angiogenic factors for prostate cancer patients following radiotherapy.[36] The study showed changes in the prostate evident of increased angiogenesis at 1-2 weeks following radiotherapy, including increased prostate perfusion (from 0.122ml/min/ml to 0.263ml/min/ml) and increased fractional vascular volume (from 13.7% to 21%), with all parameters remaining elevated at 6-12 weeks.[37]

LOCALIZATION OF PROSTATE CANCER WITH PET/CT

PET is a technique in which an image of a molecular process is obtained. For this purpose a radioactively labelled substance, a radiopharmaceutical, is administered to a patient. The substance will participate in a metabolic or (patho-)physiologic process, and accumulate at the sites the process is most active. In positron emission tomography the radioisotopes used are characterized by a surplus of positive charge in the nucleus, creating an unstable nucleus. Stability is regained by either capturing an electron (=negative charge) into the nucleus, or by emitting the surplus positive charge in the form of a positron. The positron will annihilate with an electron, generating 2 photons of energy. The radiation resulting from the annihilation event can be detected with conventional gamma-cameras, but nowadays dedicated PET-cameras are widely available. The principal difference between conventional cameras and PET-cameras is the presence of coincidence electronics. As stated, an annihilation event produces 2 photons released in opposite directions. This means that when an event is detected in a detector, the other event should be detected within a short time-frame in an opposing detector. Based on these principles modern day cameras consist of a large number of detectors with coincidence electronics, spanning an axial length of 15 cm or more. The newest cameras have detector and electronics characteristics that are thus fast that the time difference between the detection of the 2 photons can be taken into account to locate the exact position of the annihilation. These machines, so-called 'time-of-flight' machines, are undoubtedly the future of PET cameras. Together with improved image reconstruction algorithms the spatial resolution of PET will improve further.[38, 39]

In the past few years a second development occurred, that already has had great impact in clinical routine: the dual-modality PET/CT tomograph combining both PET and CT scanning in one. The functional and anatomic information offered by PET/CT is being recognized as crucial in the care of oncology patients. PET and PET/CT are playing an ever-increasing role in the management of oncologic disease. A general tendency in tracer development is the search for more specific tracers, while not losing on sensitivity. The drawbacks of such tracers problems in locating the tumour, are overcome with the new PET/CT machines. Consequently, the development of these machines itself will form a boost for radiopharmaceutical development.

The most commonly used radiopharmaceutical for PET in oncology is the glucose analogue 2-[^{18}F]fluoro-2-deoxy-d-glucose, also called fluorodeoxglucose or FDG. FDG is taken up by the cell by glucose transporters (mainly glut-1) and phosphorylised to FDG-6-phosphate by the enzyme glucose-6-phosphokinase. Whereas glucose-6-phosphate finds itself on a crossroads of a vast number of metabolic processes such is not the case of FDG-6-phophate. Because of the introduction of the fluor-atom, the three-dimensional structure of

the molecule changes after phosphorylation changes in such a way that FDG-6-phosphate is not a substrate for other enzymes anymore. As a result, the FDG is trapped in the cell, at least on the time-frame of a normal PET-scan. Unfortunately prostate cancer displays little glycolytic activity. The added effect of urinary excretion makes it very difficult to determine uptake of FDG in primary prostate cancer. Even under continuous bladder irrigation FDG was not able to distinguish between scar tissue, BPH and prostate carcinoma.[40, 41, 42] Also for restaging after local treatment FDG performed poor.[43]

PET tracers with more favourable properties have been developed and studied since. One of the most used tracers in prostate cancer is choline. Choline is one of the components of phosphatidylcholine, which in itself is an essential element of phospholipids in the cell membrane. Cancer is associated with cell proliferation and up regulation of choline kinase (the enzyme which catalyses the phosphorylation of choline), providing the rationale for the use of choline in oncological PET[44] overcome the disadvantage of the short half-life of ^{11}C-choline, several ^{18}F-labeled analogues like ^{18}F-methyl-choline and ^{18}F-ethyl-choline have been developed.

Other tracers including ^{11}C-acetate and ^{18}F- fluoro-5alpha-dihydrotestosterone are also studied in prostate cancer but limited data are available on intraprostatic tumor characterization.

^{11}C-choline has been reported first for its uptake in prostate cancer by Hara *et al*.[45] in ten patients with known prostate cancer who underwent both ^{11}C-choline PET and [18F]FDG PET. The radioactivity concentration of ^{11}C-choline in prostate cancer and metastatic sites showed a SUV > 3 in most cases. The preliminary results were validated by de Jong *et al.* in a prospective study in 25 patients with histologically proven prostate cancer and in 5 patients with benign hyperplasia.[46] The benign prostate was visualized with a mean SUV of 2.3 (range 1.3–3.2). The primary tumor could be visualized with a mean SUV of 5.0 (range 2.4–9.5) as a hot spot within the prostate gland. Five patients had proven lymph node metastases after pelvic lymph node dissection: in four of these five patients, uptake of ^{11}C-Choline in pelvic lymph nodes with metastases of 5 mm to 3 cm was seen with a mean SUV of 4.7 (range 2.9–9.1). One false positive PET was seen in a lymph node with inflammatory changes. In 19 patients without lymph node metastases, ^{11}C-choline PET was negative. Breeuwsma *et al.* studied the correlation between the uptake of choline and cell proliferation as assessed by tumour histology and Ki-67 expression.[47] This study showed no significant correlation between ^{11}C-choline uptake and Ki-67 staining. No statistically significant relationships were found between the uptake of ^{11}C-choline (SUV) and either preoperative PSA or Gleason sum score. Sutinen *et al.* evaluated the kinetics of the uptake of ^{11}C-choline in prostate cancer and benign prostatic hyperplasia.[48] The value of ^{11}C-choline PET in assessing the malignant potential of prostate tumours was analysed by correlating tracer

uptake with tumour grade, Gleason score, volume of the prostate and PSA. Fourteen patients with histologically confirmed prostate cancer and five patients with benign prostatic hyperplasia were studied with ^{11}C-choline PET. The mean Ki of untreated prostate carcinoma was 0.205±0.089 min−1 (range 0.128–0.351, including both primaries and metastases), and the mean SUV was 5.6±3.2 (range 1.9–15.5). There was a close correlation between the ^{11}C-choline influx constant and the SUV of tumours (r=0.964, P=0.0005; n=7). The mean SUV of benign prostate tissue was 3.5±1.0 (range 2.0–4.5; n=4) and the mean Ki of the benign prostate in two patients with metabolite-corrected measurement of plasma activity was 0.119± 0.076 min−1 (range 0.065–0.173). The difference between the SUVs of the prostate cancer and benign prostatic hyperplasia was not statistically significant (P=0.067). The dynamic curve of ^{11}C-choline uptake showed no apparent difference in pattern between patients with cancerous or hyperplastic tissue.

^{11}C-choline-PET/CT was studied for the detection and localization of tumors within the prostate by Farsad *et al.*[49] PET/CT findings were correlated with histopathologic analysis of the prostate using a sextant biopsy scheme in 36 patients with prostate cancer and of 5 controls. All patients underwent ^{11}C-choline PET/CT and, subsequently, radical prostatectomy with lymph node dissection. Histopathologic analysis identified cancer foci in 143 of 216 sextants biopsied. In addition, HGPIN (high-grade prostate intraepithelial neoplasm) foci were seen in 89 sextants.

At least 1 primary prostatic tumor focus could correctly be visualized through PET/CT in a total of 35 of 36 patients. On a sextant basis, PET/CT demonstrated focal ^{11}C-choline uptake in 108 sextants (50%): histologic examination showed that 94 of 108 were affected by tumor, 10 by HGPIN, 2 by HGPIN and acute prostatitis, and 2 by benign prostate hyperplasia or no pathologic findings. In sextants with areas of abnormal ^{11}C-choline uptake, the mean SUV was 5.3 ± 2.2 (range, 2.2–12) and the mean T/B ratio was 2.0 ± 0.5 (range, 1–3.4). PET/CT found 108 sextants without evidence of abnormal ^{11}C-choline uptake. These findings were true negative in 59 of the sextants and false negative in 49; in those 49, histologic examination proved the presence of cancer foci. PET/CT had a sensitivity of 66%, a specificity of 81%, an accuracy of 71%, a positive predictive value of 87%, and a negative predictive value of 55%.

No statistically significant difference was found between tumors and HGPIN using either SUV or T/B ratio. The SUV range measured for cancer foci reflects the heterogeneity of prostate cancer which could explain the failure to detect all cancer foci. Both conditions (small dimension and low uptake) could explain the high rate of false-negative results with ^{11}C-choline PET/CT. The study also demonstrated that HGPIN can accumulate ^{11}C-choline. As HGPIN and carcinoma have a strong tendency to be present simultaneously and exhibit the same “zonal” origin and anatomic proximity, a possible explanation for pathologic uptake

of ^{11}C-choline in sextants with HGPIN foci could be that some of these regions harboured a small focus of cancer undetected by pathologists. The complete overlap of SUV and T/B ratio between cancer foci and HGPIN foci detected by PET/CT supported this hypothesis and pointed out that no single SUV or T/B ratio cut-off can differentiate between cancer and HGPIN.

In a clinical study by Martorana *et al.* the sensitivity of ^{11}C-choline-PET/CT for intraprostatic localization of primary prostate cancer on a nodule-by-nodule basis was assessed, and compared with histology using a 12-core transrectal biopsy scheme and post prostatectomy.[50] In 43 patients with known prostate cancer who had received ^{11}C-choline PET/CT before initial biopsy, they evaluated sensitivity of ^{11}C-choline-PET/CT for localization of nodules 5 mm or greater using radical prostatectomy histopathology as the reference standard.

All 43 patients showed 1 or more focal uptake (total 70); focal uptake was bilateral in 32 (74%) patients and unilateral in 11 (26%). In 8 patients focal uptake was recorded in the presence only of high grade PIN. At nodule assessment 57/70 instances of focal uptake were in correspondence with the histopathologically identified nodules 5 mm or greater in diameter, corresponding to a sensitivity of 83% for localization of tumor nodules. PET/CT detected only 1 of 23 (4%) cancer focus 5 mm or less. At sextant PET/CT had slightly better sensitivity than transrectal ultrasound guided biopsy (66% vs 61%, p=0.434) but was less specific (84% vs 97%, p=0.008).

Testa *et al.* retrospectively compared sensitivity and specificity of magnetic resonance (MR) imaging, three-dimensional (3D) MR spectroscopy, combined MR imaging and 3D MR spectroscopy, and ^{11}C-choline PET/CT for intraprostatic tumor sextant localization in 26 men with prostate cancer who underwent radical prostatectomy.[51] Sensitivity, specificity, and accuracy of PET/CT were 55%, 86%, and 67% respectively, versus 54%, 75%, and 61% for MR imaging and 81%, 67%, and 76% for 3D MR spectroscopy. Sensitivity of PET/CT improved using a quantitative analysis using the maximum SUV threshold of 2.9 or higher. Sensitivity was increased to 72% reducing specificity to 65%. ^{11}C-choline PET/CT demonstrated a lower sensitivity compared to both 3D MR spectroscopic imaging alone or to combined MR imaging and 3D MR spectroscopic, with a comparable specificity.

The current literature on intra prostatic localization of recurrent prostate cancer is limited. ^{11}C-choline PET showed to be a sensitive technique in localization of the site of recurrence after EBRT (either local, regional or distant) in a prospective cohort study by Breeuwsma *et al.*[52] The overall concordance of PET with a local recurrence was 88 % using a composite reference with histology and clinical follow up after local salvage treatment. The concordance of the intra prostatic distribution of the tumor with PET with histology from serial biopsies was 47% (7/15) in unilateral cases and 41% (11/27) in bilateral cases (Figure 3)

(Rybalov *et al.*, unpublished data). This could in part be due to sampling errors using sextant biopsies. Whole mount correlation studies showing the accuracy of ^{11}C-choline PET/CT for intra prostatic localization of recurrent prostate cancer are also lacking at the time of this review.

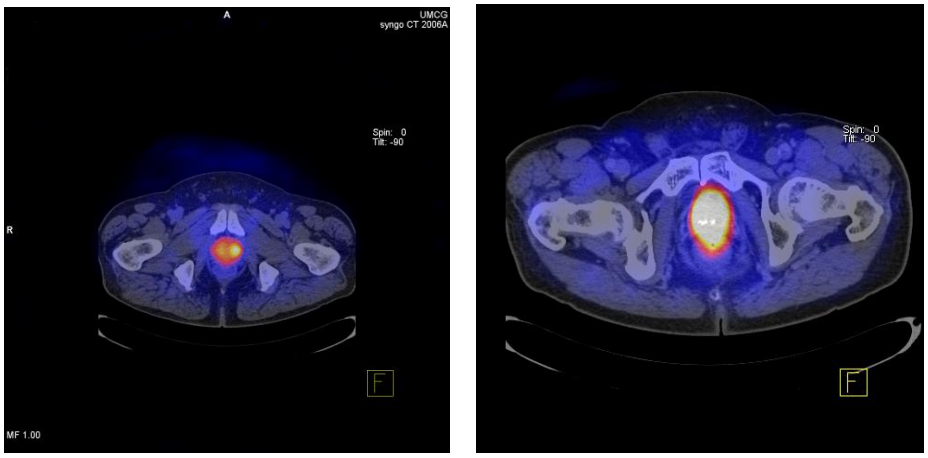

A **B**

Fig 3 ^{11}C-choline PET/CT

On the left a case with focal uptake of choline in a patient with a Gleason 7 (4+3) tumor in the left lobe in all four biopsies and a Gleason 7 (3+4) in 20% of the biopsies in the right lobe. On the right a case with diffuse uptake of choline in a patient with a Gleason 8 (4+4) tumor in the left lobe in all four biopsies and a Gleason 7 (3+4) in all four biopsies in the right lobe.

CONCLUSION

Conventional CT and FDG PET are not able to detect prostate cancer foci <5mm within the prostate. Based on the preliminary studies, DCE-CT may be a useful tool in for localization of prostate tumours and perhaps more importantly, quantification of therapeutic response in prostate cancer. However validation work is required to define its accuracy and role in therapeutic paradigms such as focal therapies, particularly given the current accuracy of MRI. In the future, combining DCE-CT with CT or ^{11}C-choline PET/CT may be an alternative to MRI, offering a combination of quantitative parameters which may correlate to tumour prognosis as well as cancer localization for focal therapy.

REFERENCES

1. Heidenreich A, Aus G, Abbou CC, et al.: Guidelines on Prostate Cancer, European Association of Urology, 2007, pp 1-114.
2. Platt J, Bree R, Schwab R. The accuracy of CT in the staging of carcinoma of the prostate. Am J Roentgenol 1987;149:315-318.
3. Golimbu M, Morales P, Al-Askari S, et al. Cat scanning in staging of prostatic cancer. Urology 1981;18:305-308.
4. Oyen R, Van Poppel H, Ameye F, et al. Lymph node staging of localized prostatic carcinoma with CT and CT- guided fine-needle aspiration biopsy: prospective study of 285 patients. Radiology 1994;190:315-322.
5. Thompson I, Thrasher JB, Aus G, et al.: Guideline for the Management of Clinically Localized Prostate Cancer: 2007 Update, American Urological Association, 2007, pp 1-82.
6. Kumada M, Gomi K, Kozuka T, et al. Inter/Intra-fractionation Prostate Motion Evaluated with Multiple CT Scans during a Course of External Beam Radiation Therapy. ASTRO 2008; Boston. American Society for Therapeutic Radiology and Oncology. Abstract 2359.
7. Peng C, Kainz K, Lawton C, et al. CT versus Ultrasound Image Guided Prostate Cancer Radiotherapy: dosimetric impacts. ASTRO 2007; Los Angeles. American Society for Therapeutic Radiology and Oncology. Abstract 2967.
8. Jang S, Hurley AA, Curran BH, et al. Use of Cone-beam CT in Prostate IMRT. ASTRO 2008; Boston. American Society for Therapeutic Radiology and Oncology. Abstract 2907.
9. Kane CJ, Amling CL, Johnstone PAS, et al. Limited value of bone scintigraphy and computed tomography in assessing biochemical failure after radical prostatectomy. Urology 2003;61:607-611.
10. Yu KK, Hricak H. Imaging Prostate Cancer. Radiologic Clinics of North America 2000;38:59-85.
11. Goh V, Padhani A. Imaging tumor angiogenesis: functional assessment using MDCT or MRI? Abdominal Imaging 2006;31:194-199.
12. Cuenod C, Fournier L, Balvay D, et al. Tumor angiogenesis: pathophysiology and implications for contrast-enhanced MRI and CT assessment. Abdominal Imaging 2006;31:188-193.
13. Padhani AR, Harvey CJ, Cosgrove DO. Angiogenesis imaging in the management of prostate cancer. Nat Clin Pract Urol 2005;2:596-607.

14. Engelbrecht MR, Huisman HJ, Laheij RJF, et al. Discrimination of Prostate Cancer from Normal Peripheral Zone and Central Gland Tissue by Using Dynamic Contrast-enhanced MR Imaging1. Radiology 2003;229:248-254.
15. Fütterer JJ, Heijmink SWTPJ, Scheenen TWJ, et al. Prostate Cancer Localization with Dynamic Contrast-enhanced MR Imaging and Proton MR Spectroscopic Imaging1. Radiology 2006;241:449-458.
16. Fütterer JJ, Engelbrecht MR, Huisman HJ, et al. Staging Prostate Cancer with Dynamic Contrast-enhanced Endorectal MR Imaging prior to Radical Prostatectomy: Experienced versus Less Experienced Readers1. Radiology 2005;237:541-549.
17. Hara N, Okuizumi M, Koike H, et al. Dynamic contrast-enhanced magnetic resonance imaging (DCE-MRI) is a useful modality for the precise detection and staging of early prostate cancer. The Prostate 2005;62:140-147.
18. Prando A, Wallace S. Helical CT of Prostate Cancer: Early Clinical Experience. Am J Roentgenol 2000;175:343-346.
19. Mahmood S, Hoe J: Emerging Role of Multi-detector CT Imaging: Integrating Cardiology for Nuclear Medicine Physicians, 2009, pp 163-176.
20. Martin DR, Semelka RC. Health effects of ionising radiation from diagnostic CT. The Lancet 2006;367:1712-1714.
21. Brenner DJ, Hall EJ. Computed Tomography -- An Increasing Source of Radiation Exposure. N Engl J Med 2007;357:2277-2284.
22. Harrison RM, Wilkinson M, Shemilt A, et al. Organ doses from prostate radiotherapy and associated concomitant exposures. Br J Radiol 2006;79:487-496.
23. Jeukens CRLPN, Berg CATvd, Donker R, et al. Feasibility and measurement precision of 3D quantitative blood flow mapping of the prostate using dynamic contrast-enhanced multi-slice CT. Physics in Medicine and Biology 2006;51:4329-4343.
24. Henderson E, Milosevic MF, Haider MA, et al. Functional CT imaging of prostate cancer. Physics in Medicine and Biology 2003;48:3085-3100.
25. Marcus CD, Ladam-Marcus V, Cucu C, et al. Imaging techniques to evaluate the response to treatment in oncology: Current standards and perspectives. Critical Reviews in Oncology/Hematology 2008;In Press, Corrected Proof:
26. Cenic A, Nabavi DG, Craen RA, et al. Dynamic CT Measurement of Cerebral Blood Flow: A Validation Study. AJNR Am J Neuroradiol 1999;20:63-73.
27. Purdie TG, Henderson E, Lee T-Y. Functional CT imaging of angiogenesis in rabbit VX2 soft-tissue tumour. Physics in Medicine and Biology 2001;3161.
28. Gillard J, Minhas P, Hayball M, et al. Assessment of quantitative computed tomographic cerebral perfusion imaging with H2(15)O positron emission tomography. Neurological Research 2000;22:457-464.

29. Tateishi U, Kusumoto M, Nishihara H, et al. Contrast-enhanced dynamic computed tomography for the evaluation of tumor angiogenesis in patients with lung carcinoma. Cancer 2002;95:835-842.
30. Wang JH, Min PQ, Wang PJ, et al. Dynamic CT Evaluation of Tumor Vascularity in Renal Cell Carcinoma. Am J Roentgenol 2006;186:1423-1430.
31. Haider MA, Milosevic M, Fyles A, et al. Assessment of the tumor microenvironment in cervix cancer using dynamic contrast enhanced CT, interstitial fluid pressure and oxygen measurements. International Journal of Radiation Oncology*Biology*Physics 2005;62:1100-1107.
32. Miles KA, Griffiths MR. Perfusion CT: a worthwhile enhancement? Br J Radiol 2003;76:220-231.
33. Bates TS, Gilllatt DA, Cavanagh PM, et al. A comparison of endorectal magnetic resonance imaging and transrectal ultrasonography in the local staging of prostate cancer with histopathological correlation. British Journal of Urology 1997;79:927-932.
34. May F, Treumann T, Dettmar P, et al. Limited value of endorectal magnetic resonance imaging and transrectal ultrasonography in the staging of clinically localized prostate cancer. BJU International 2001;87:66-69.
35. St. Lawrence KS, Lee T-Y. An Adiabatic Approximation to the Tissue Homogeneity Model for Water Exchange in the Brain: I. Theoretical Derivation. J Cereb Blood Flow Metab 1998;18:1365-1377.
36. Harvey CJ, Blomley MJK, Dawson P, et al. Functional CT Imaging of the Acute Hyperemic Response to Radiation Therapy of the Prostate Gland: Early Experience. Journal of Computer Assisted Tomography 2001;25:43-49.
37. Harvey C, Dooher A, Morgan J, et al. Imaging of tumour therapy responses by dynamic CT. European Journal of Radiology 1999;30:221-226
38. Surti S, Kuhn A, Werner ME, et al. Performance of Philips Gemini TF PET/CTscanner with special consideration for its time-of-flight imaging capabilities.J Nucl Med 2007; 48:471–480.
39. Rizzo G, Castiglioni I, Russo G, et al. Using deconvolution to improve PET spatial resolution in OSEM iterative reconstruction. Methods Inf Med 2007;46:231–235.
40. Effert PJ, Bares R, Handt S, et al. Metabolic imaging of untreated prostate cancer by positron emission tomography with 18fluorine-labeled deoxyglucose. J Urol 1996;155:994-998.
41. Laubenbacher C, Hofer C, Avril N, et al. F-18 FDG PET for differentiation of local recurrent prostate cancer and scar. J Nucl Med 1995;36(SUPPL):198P.
42. Shreve PD, Grossman HB, Gross MD, et al. Metastatic prostate cancer: initial findings of PET with 2-deoxy-2-[F-18]fluoro-D-glucose. Radiology 1996;199:751-756.

43. Picchio M, Messa C, Landoni C et al. Value of 11C choline-positron emission tomography for restaging prostate cancer: a comparison with 18F fluorodeoxyglucose-positron emission tomography. J Urol 2003;169:1337–40.
44. Katz-Brull R, Degani H. Kinetics of choline transport and phosphorylation in human breast cancer cells; NMR application of the zero trans method. Anticancer Res 1996;16:1375-1380.
45. Hara T, Kosaka N, Kishi H. PET imaging of prostate cancer using carbon-11-choline. J Nucl Med 1998;39:990-995.
46. de Jong IJ, Pruim J, Elsinga PH, et al. Visualization of prostate cancer with 11C-choline positron emission tomography. Eur Urol 2002;42:18-23.
47. Breeuwsma AJ, Pruim J, Jongen MM, et al. In vivo uptake of [11C]choline does not correlate with cell proliferation in human prostate cancer. Eur J Nucl Med Mol Imaging 2005;32:668-673.
48. Sutinen E, Nurmi M, Roivainen A, et al. Kinetics of [(11)C]choline uptake in prostate cancer: a PET study. Eur J Nucl Med Mol Imaging 2004;31:317-324.
49. Farsad M, Schiavina R, Castellucci P, et al. Detection and localization of prostate cancer: correlation of (11)C-choline PET/CT with histopathologic step-section analysis. J Nucl Med 2005;46:1642-1649.
50. Martorana G, Schiavina R, Corti B, et al. 11C-choline positron emission tomography/computerized tomography for tumor localization of primary prostate cancer in comparison with 12-core biopsy. J Urol 2006;176:954-960; discussion 60.
51. Testa C, Schiavina R, Lodi R, et al. Prostate cancer: sextant localization with MR imaging, MR spectroscopy, and 11C-choline PET/CT. Radiology 2007;244:797-806.
52. Breeuwsma AJ, Leliveld AM, Pruim J, et al. Detection of local, regional and distant recurrence in patients with PSA relapse after external beam radiotherapy using 11C-choline positron emission tomography (PET). IJROBP 2009 (article in press).